

# A Compact 2-18 GHz Halved Vivaldi Antenna

Ping Wang<sup>1,2</sup>, Guangjun Wen<sup>1</sup>, Yongjun Huang<sup>1</sup>, and Haobin Zhang<sup>3</sup>

<sup>1</sup>Centre for RFIC and System Technology  
School of Communication and Information Engineering  
University of Electronic Science and Technology of China, Chengdu 611731, China  
wangpingcqz@163.com

<sup>2</sup>College of Electronic and Information Engineering  
Chongqing Three Gorges University, Chongqing 404000, China

<sup>3</sup>Science and Technology on Electronic Information Control Laboratory  
Chengdu 610036, China

**Abstract** — A compact, broadband, halved planar Vivaldi antenna has been proposed in this paper. The halved Vivaldi antenna is located on a large metal plane vertically, and connected to the metal plane through feed-line and short-line. The proposed antenna was designed, fabricated, and tested. Experimental and simulated results show that the proposed halved Vivaldi antenna has a wide bandwidth from approximately 1.44 to 18.5 GHz, and a small size of only 30 mm × 60.5 mm. Moreover, the designed antenna can provide excellent characteristics, including directive radiation characteristics and vertically polarized radiation pattern. These results prove that the proposed antenna should be useful in many metal surface-mounted communication systems, such as missile, unmanned aerial vehicles, and the like.

**Index Terms** — Metal plane, small size, ultra-wide bandwidth antenna, Vivaldi antenna.

## I. INTRODUCTION

Tapered Slot Antennas (TSA), as its name suggests, is a class of antenna with tapered radiation slot-line and can be classified into different types according to its tapered curves, such as, linear TSA [1,2], constant width TSA [3], logarithmically TSA [4], exponentially TSA or Vivaldi antenna [5-9], and so on. The Vivaldi Tapered Slot Antenna (TSA) consists of an exponentially tapered slot cut in a metal film (with

or without a thin substrate) on one side of the material, which flares from a small slot ( $50 \Omega$ ) to a large opening notch, matching to free space's wave impedance of  $377 \Omega$ . It is normally fabricated by cutting a narrow slot in continuous metal film and the other end of the slot is connected by a quarter-wave cavity to improve its impedance matching and forward gain. A transmission line is placed on the other side of the substrate, and one end of that is connected with a quarter-wave micro-strip line cross over transition [10], which excites a circular or rectangular cavity on the slot side. The energy from this cavity is transferred to the slot-line taper, and propagating along the slot, radiates in the end-fire direction. To enhance the impedance bandwidths, the quarter-wave micro-strip line is generally replaced by the feed technique of a micro-strip fan-shaped stub [11]. However, a micro-strip fan-shaped stub produces very high radiation loss and even distorts radiation patterns; especially in a high frequency range, which limits its applications in some systems. To reduce the dissipative losses and unwanted radiation from the balun, it is necessary to seek for a new balun and then assemble it with tapered slot. In recent publications, two different planar fourth-order Marchand baluns were introduced [12,13], which reduce the physical size of the balun components and unwanted radiation. However, they have complex structure and narrower impedance bandwidths, and also depend on high permittivity

dielectric. Therefore, simple configuration and wide bandwidth are desirable.

On the other hand, it is commonly known that single Vivaldi antenna works best when it is more than one wavelength long and the height of the antenna aperture is greater than one-half wavelength referring to the lowest resonant frequency [11], which means that the antenna still has large dimension for some limited communication space, so it is a challenging task to minimize the physical size of Vivaldi antenna without simultaneously reducing the bandwidths. In this letter, we present a compact halved Vivaldi antenna. The proposed antenna with a compact size of only  $30 \text{ mm} \times 60.5 \text{ mm}$  ( $0.144 \lambda_0 \times 0.29 \lambda_0$ , where  $\lambda_0$  is the maximum working wavelength) offers a bandwidth from 1.44 to 18.5 GHz, and also possesses directive radiation patterns and low cross-polarization levels; which is very suitable for mounting on metallic surface of a variety of communication systems. Simulated and measured results show that the antenna has very wide frequency bandwidth, directive radiation patterns, small size and vertically polarized characteristics.

## II. ANTENNA CONFIGURATION

The geometrical configuration of the proposed antenna is shown in Fig. 1. The antenna has a double-layer metallic structure and is printed on a substrate of thickness of 0.5 mm, with the dielectric constant of 3.55. In order to reduce the size and increase the bandwidth of the antenna, a resistor of  $R=100 \ \Omega$  is integrated at the slot-line end of the proposed antenna. A  $50 \ \Omega$  SMA connector is used as the feed source, whose inner conductor is directly soldered to one end of the feed-line, and the outer conductor is connected directly to the metal plane. In this design, the other end of feed-line is shorted to the metal surface of the antenna by metalized vias. The outer edge and inner edge taper of the proposed antenna are described by the mathematical exponential functions, which are defined as:

$$\begin{aligned} x_i &= c_1 \exp(R_1 z) + c_2, \\ x_o &= \exp(R_2 z \wedge sf) + c_3, \end{aligned} \quad (1)$$

where  $c_1=(2w_1-w_0)/(2(\exp(R_1 L_1)-1))$ ,  $R_1=0.07$ ,  $c_2=(w_0 \exp(R_1 L_1)-2w_1)/(2(\exp(R_1 L_1)-1))$ ,  $sf=1.65$ ,  $c_3=(c_1 \exp(R_1 L_1)+c_2)+m-m_1$ ,  $R_2=0.06$ ,  $x_i$  and  $x_o$  denote the distances from the slot center line to the inner and outer edges, respectively. Thus, the end-

point  $z$ -value of the outer exponential curve ( $P$ ) can be expressed as:

$$P = \left( \ln \frac{c_1 \exp(R_1 L_1) + c_2 + m + 1 - c_3}{R_2} \right) \wedge \left( \frac{1}{sf} \right). \quad (2)$$

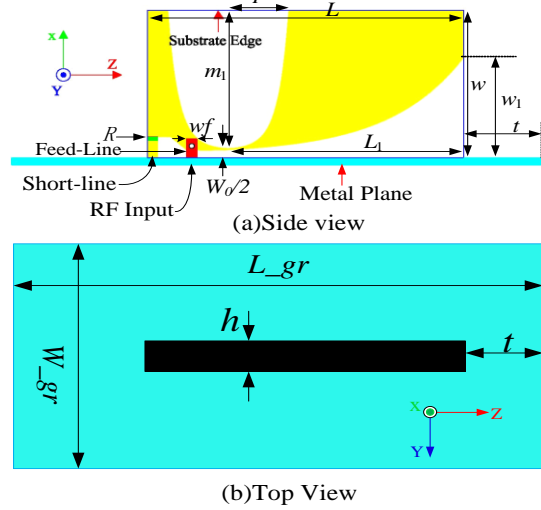


Fig. 1. Configuration of the proposed antenna.

The proposed antenna is located above a metal plane of size  $W_{gr} \times L_{gr}$  ( $200 \text{ mm} \times 200 \text{ mm}$ ), which is large enough for reducing the effect of SMA connector, and the top edge of that keeps a distance  $t$  from the edge of the metal plane. The proposed structure is optimized by using Ansoft High Frequency Structure Simulator (HFSS) and the optimized values are illustrated in Table 1.

Table 1: Parameters of the antenna as Fig. 1

Parameter	$m_1$	$wf$	$w_0$
Value (mm)	29.5	2	0.5
Parameter	$L_1$	$L$	$t$
Value (mm)	45	60.5	0
Parameter	$w$	$w_1$	$m$
Value (mm)	30	20	$w-w_1$

## III. SIMULATED AND MEASURED RESULTS

To validate the design concept, the prototype of the halved planar Vivaldi antenna was fabricated and tested. Measured and simulated VSWR for the proposed antenna are shown in Fig. 2, which presents a little discrepancy owing to the error of substrate parameters and tolerance in manufacturing. It is observed from Fig. 2 that the measured VSWR is less than 2.2 over the

frequency ranges of approximately 1.44-18.5 GHz (12.9:1), which almost satisfies the bandwidth requirement of 2-18 GHz. Radiation characteristics of the proposed antenna are also considered. The far-field radiation patterns of the proposed antenna in E-plane ( $xz$ -plane) and H-plane ( $yz$ -plane) for both  $E_\phi$  and  $E_\theta$  at frequencies of 2 GHz, 6 GHz and 10 GHz, are shown in Fig. 3. The measured patterns in general agree well with the simulated results. It is seen that the proposed antenna has directive radiation characteristics, and in E-plane the cross-polarization levels are 20 dB less than co-polarization levels. However, in H-plane, the cross-polarization curve has a deep depression in end-fire direction, which shows that the antenna has a high polarization ratio in end-fire direction, and in other directions the cross-polarization levels keep varying around -20 dB. It is also noticed that in E-plane, as the frequency is increased, the effective radiation area is far away from the edge of the metal plane; thus, the main beam direction

angle also increases, and when the frequency is increased continuously, the main beam direction angle keeps a maximum value of 30 degrees but a side lobe will be appeared in the close proximity of major lobe which varies from 65 to 80 degrees.

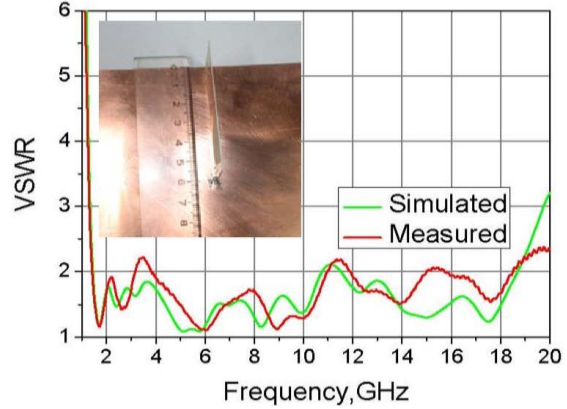


Fig. 2. Simulated and measured VSWR for the proposed antenna.

Frequency ( $f$ )	Simulated Radiation Pattern		Measured Radiation Pattern	
	E-plane ( $xz$ -plane)	H-plane ( $yz$ -plane)	E-plane ( $xz$ -plane)	H-plane ( $yz$ -plane)
2 GHz				
6 GHz				
10 GHz				

Fig. 3. Normalized radiation pattern of the proposed antenna ( —  $E_\phi$ ; —  $E_\theta$  ).

With the help of the simulator HFSS, we can further study surface current distributions of the proposed antenna at two resonant frequencies (1.7 GHz and 5.8 GHz), which are presented in Fig. 4. It is seen clearly that at 1.7 GHz the main current

distributions are concentrated on the radiation slot-line and the end of slot-line, but for the other frequency the dominated current only flows along tapered slot, which proves the method of enhancing the bandwidth. It should be noticed that

Table 2 summarizes the performance comparison with other works [1,2,4,7] in terms of dielectric constant, size, operating frequency ranges, and bandwidth. By examining all the available low-profile tapered slot antennas, it was found that these designs are either using notched slot [2] which produces band-rejection in high frequency and can not extend higher working frequency ranges, or having larger size which is greater than  $80 \times 140 \text{ mm}^2$  as in [4,7] or inadequate operating frequency ranges [1]. However, the proposed antenna not only has smaller size, but also has wider bandwidth.

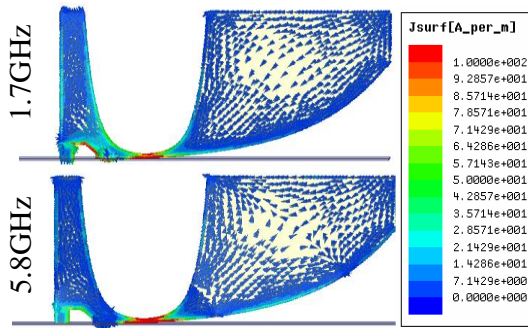


Fig. 4. Simulated current distributions of the proposed antenna at two lowest resonant frequencies.

Table 2: Performance comparison

Works	$\epsilon_r$	Dimension (mm <sup>2</sup> )	Operating Frequency	Impedance Bandwidth
Ref. [1]	2.65	18×23	6.2-12.3 GHz	6.1 GHz
Ref. [2]	4.55	35×36	3.1-10.6 GHz	7.5 GHz
Ref. [4]	2.65	170×300	0.89-13.8 GHz	12.91 GHz
Ref. [7]	4.4	80×140	1.8-14 GHz	12.2 GHz
This work	3.55	30×60.5	1.44-18.5 GHz	17.06 GHz

#### IV. PARAMETRIC STUDIES

In this section, parametric studies of the proposed antenna are presented to provide more detailed information about the antenna design and optimization. The parameters under study include the resistance value  $R$ , the substrate thickness  $h$ , length of radiation slot-line  $L_1$ , height of radiation slot-line  $w_1$ , and distance away from the edge of

ground plane  $t$ . To better understand the influence of the parameters on the performance of the antenna, only one parameter at a time will be varied, while others are kept unchanged unless especially indicated.

#### A. Resistance value ( $R$ )

To further enhance the bandwidth of the antenna, a resistor  $R$  is integrated at slot-line end of the antenna. Figure 5 shows the reflection coefficient curves for different values of  $R$ : 0  $\Omega$ , 50  $\Omega$ , 100  $\Omega$ , 200  $\Omega$ , and 500  $\Omega$ . It is clearly observed that the variation of the values of  $R$  has a significant effect on the reflection coefficient, especially in low frequency. As the figure describes, when the value of  $R$  is equal to zero, namely terminal patch shorted to the ground plane, the lowest resonant frequency is 2.72 GHz. However, as the resistor value of  $R$  becomes 100  $\Omega$ , the lowest resonant frequency becomes 1.5 GHz. If the value of  $R$  is increased continuously, such as to 500  $\Omega$ , the resonant frequency will be disappeared. This is owing to the current path extended as a resistor introduced, and an extra resonant mode is added in low frequency resulting in enhanced bandwidth, which seems to reasonably agree with surface current results shown in Fig. 4. For high frequency bands, the variation of  $R$  has minor effect on reflection coefficient value. Hence, to have a wider bandwidth, the resistance value  $R$  is selected as 100  $\Omega$ . It must be pointed out that the wider bandwidth is achieved due to not only the suitable resistance value, but also the dual-exponential edges configuration selected for smaller quality factor.

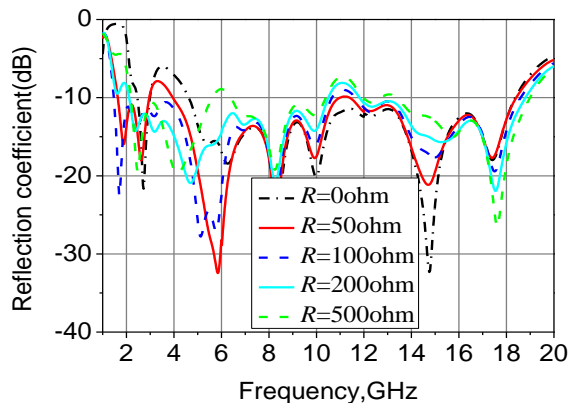


Fig. 5. Simulated reflection coefficient performances as a function of  $R$ .

### B. Substrate thickness ( $h$ )

The effect of varying substrate thickness  $h$  on the antenna reflection coefficient is shown in Fig. 6. It is seen clearly from the figure that distance  $h$  has significant effect on the bandwidth of the antenna. With increasing  $h$ , the bandwidth is gradually decreased and cannot fully cover 1.5-18 GHz band. Hence, to have a wider impedance bandwidth, the distance  $h$  should be chosen as 0.5 mm.

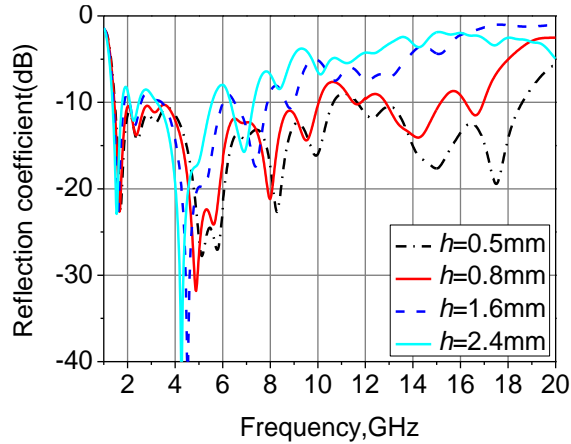


Fig. 6. Simulated reflection coefficient performances as a function of substrate thickness ( $h$ ).

### C. Length of radiation slot-line ( $L_1$ )

Figure 7 shows the effect of length  $L_1$  of tapered slot line on reflection coefficient. The figure shows that with increasing  $L_1$  from 40 mm to 65 mm, the reflection coefficient curves in low frequency bands have larger changes than that in high frequency bands. As depicted in Fig. 7, when the length  $L_1$  is equal to 40 mm or 45 mm, the lowest resonant frequency occurs at 1.5 GHz; nevertheless, a stop-band is presented in low frequency as the length  $L_1$  arrives at 55 mm and 65 mm (i.e., 2.8 GHz and 2.45 GHz, respectively). Figure 8 demonstrates the impact of varying the design parameter  $L_1$  on the radiation pattern of the

proposed antenna. It is seen clearly from the figure that for same frequency with increasing the length  $L_1$ , the proposed antenna keeps low cross-polarized levels, generally less than -20 dB at end-fire direction in E-plane ( $xz$ -plane) and H-plane ( $yz$ -plane), and the cross-polarized level in E-plane is lower than that in H-plane. It is also noticed that the radiation pattern is similar to monopole-like radiation at 2 GHz; in other words, the co-polarized pattern has two relative minimum points in  $x$ -axis to form a horizontal eight-shaped radiation pattern in E-plane and co-polarized pattern in H-plane keeps nearly omni-directional radiation pattern, which shows that the proposed antenna has vertical polarization characteristics. However, for same length  $L_1$ , as frequency increases the main beam direction angle deviates from the  $z$ -axis and keeps the angle in 30 degrees, but when the working frequency exceeds 10 GHz the side lobe peak value will be increased, and the higher the frequency, more the side lobe will be. This behavior is largely due to the resonant slot working in high frequency away from the edge of ground plane, which leads to the radiant electromagnetic waves hardly crossing over the metal plane.

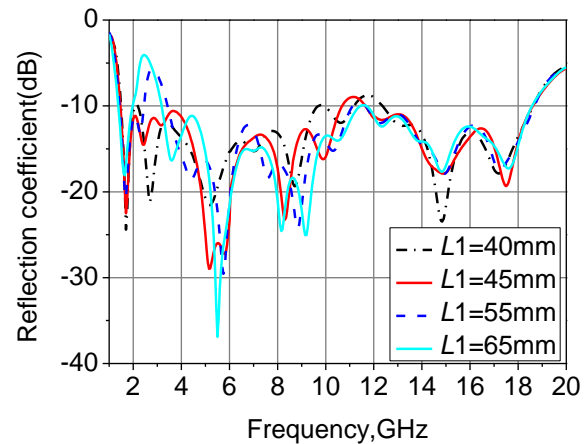


Fig. 7. Effect of length  $L_1$  of radiation slot-line on the reflection coefficient.

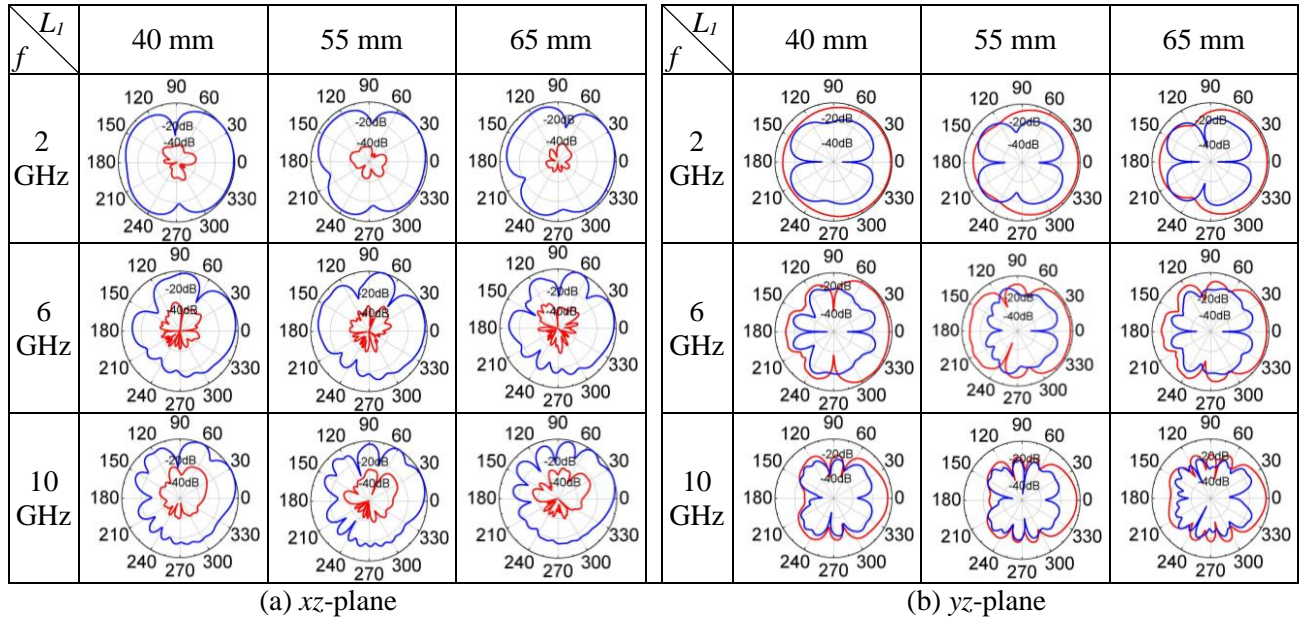


Fig. 8. Effect of length  $L_1$  of tapered slot line on the radiation pattern (—  $E_\phi$ ; —  $E_\theta$ ).

#### D. Width of radiation slot-line ( $w_1$ )

In this part of parametric studies, we change the height  $w_1$  of antenna aperture to show effects of aperture dimensions on the reflection coefficient and radiation pattern. Figure 9 shows the simulation results for various values of aperture height when other parameters keep invariable. It can be seen that aperture height has larger effect on the reflection coefficient in low frequency bands than that in high frequency bands, and with increasing  $w_1$ , the lowest resonant frequency is shifted downward and vice versa. On the other hand, Fig. 10 shows the effect of variation of height  $w_1$  on the radiation pattern. It is found that in E-plane ( $xz$ -plane) when the height  $w_1$  is increased, the radiation pattern keeps monopole-like radiation at 2 GHz. It is also observed from the E-plane figure that for same aperture height  $w_1$ , with increasing frequency more minimum point of co-polarized pattern is also produced to form many side lobes, peak value of which is nearly equal to that of main beam, and the main beam directional angle measured from the  $z$ -axis increases (i.e., 30 degrees at 10 GHz). However, in H-plane, the co-polarized pattern almost remains unchanged when the height  $w_1$  is varied, and for same height  $w_1$ , with increasing frequency the co- and cross-

polarized patterns present random variation but the main beam direction of co-polarized pattern is always directed to  $z$ -axis and the cross-polarized pattern shows eight-shaped curve, the minimum point value of cross-polarized pattern is also increased. Note, that as the height  $w_1$  is increased from 15 mm to 30 mm, the antenna also keeps low cross-polarization level with less than -20 dB at end-fire direction in both principal planes.

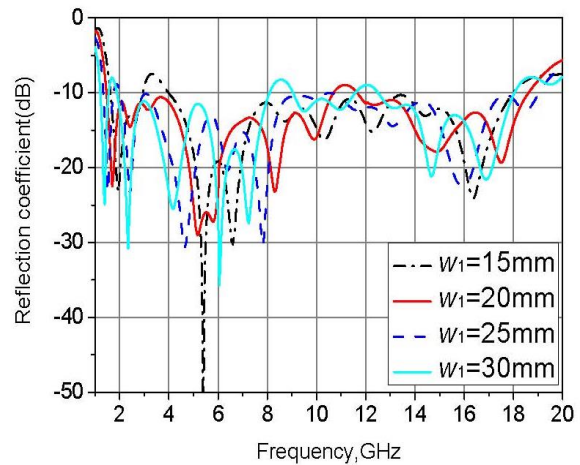


Fig. 9. Effect of height  $w_1$  of antenna aperture on the reflection coefficient.

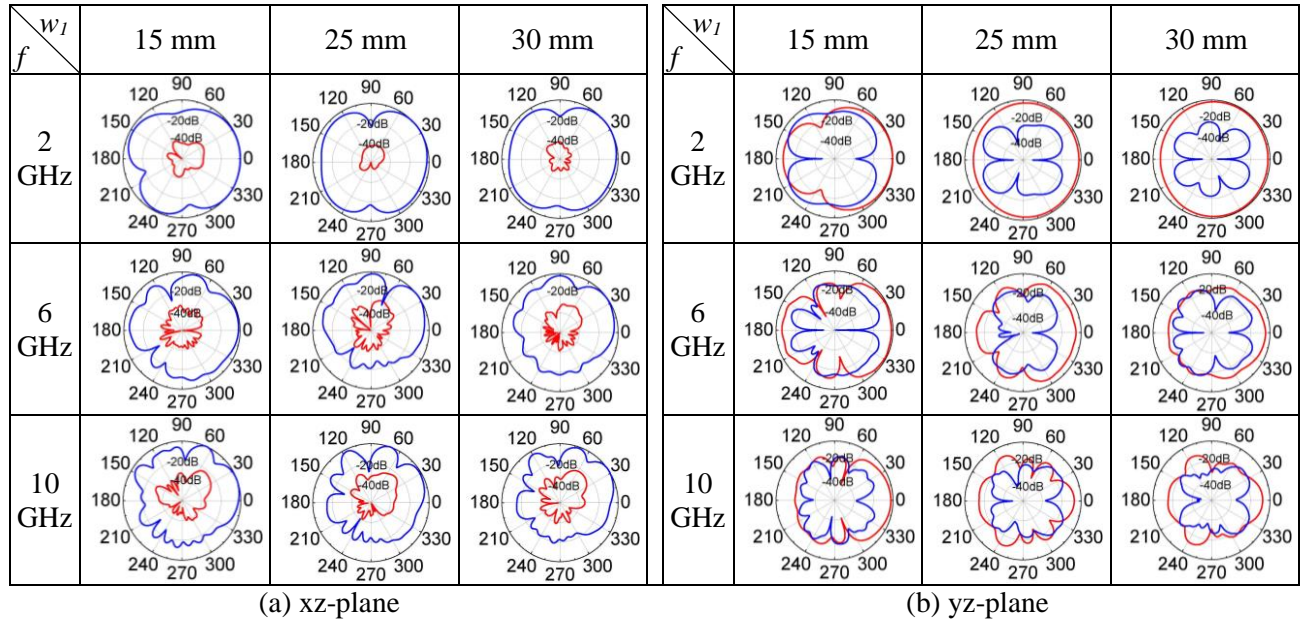


Fig. 10. Effect of height  $w_1$  of antenna aperture on radiation pattern (—  $E_\phi$ ; —  $E_\theta$ ).

**E. Distance away from the edge of ground plane**

To further know antenna performance, this section presents the effect of the variation of distance  $t$  on the reflection coefficient and radiation pattern. Figure 11 presents the effect of distance  $t$  on reflection coefficient. It is seen clearly that with variation of distance  $t$ , the reflection coefficient curves keep nearly invariable. Figure 12 demonstrates the impact of varying the parameter  $t$  on the radiation pattern of the proposed antenna. It is observed that for same working frequency as the distance  $t$  increases, the main beam direction angle of co-polarized pattern measured from the  $z$ -axis increases in E-plane; such as, at 2 GHz when distance  $t$  is equal to 5 mm, the main beam will be directed to  $z$ -axis, but when distance  $t$  is increased to 30 mm, the angle between main beam and  $z$ -axis is 30 degrees. If the distance  $t$  is increased continuously up to 50 mm, the main beam angle always remains at 30 degrees. Moreover, as the distance  $t$  keeps unchanged with increasing frequency, the side lobes are appeared in the close proximity of major lobe, and the higher the frequency, more the side lobe will be. As the frequency increases continuously, the main beam angle remains unchanged while the distance

$t$  is varied from 5 to 50 mm. However, in H-plane, with increasing distance  $t$ , the co-polarized pattern almost keeps same shaped curve and cross-polarized pattern is also changed a little. It has been found that the variation of distance  $t$  has larger effect on E-plane radiation pattern as compared to the effect on the H-plane radiation pattern and the reflection coefficient.

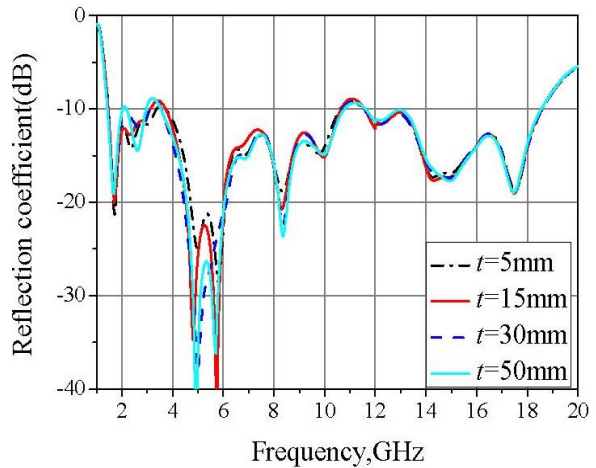


Fig. 11. Effect of distance  $t$  on reflection coefficient.

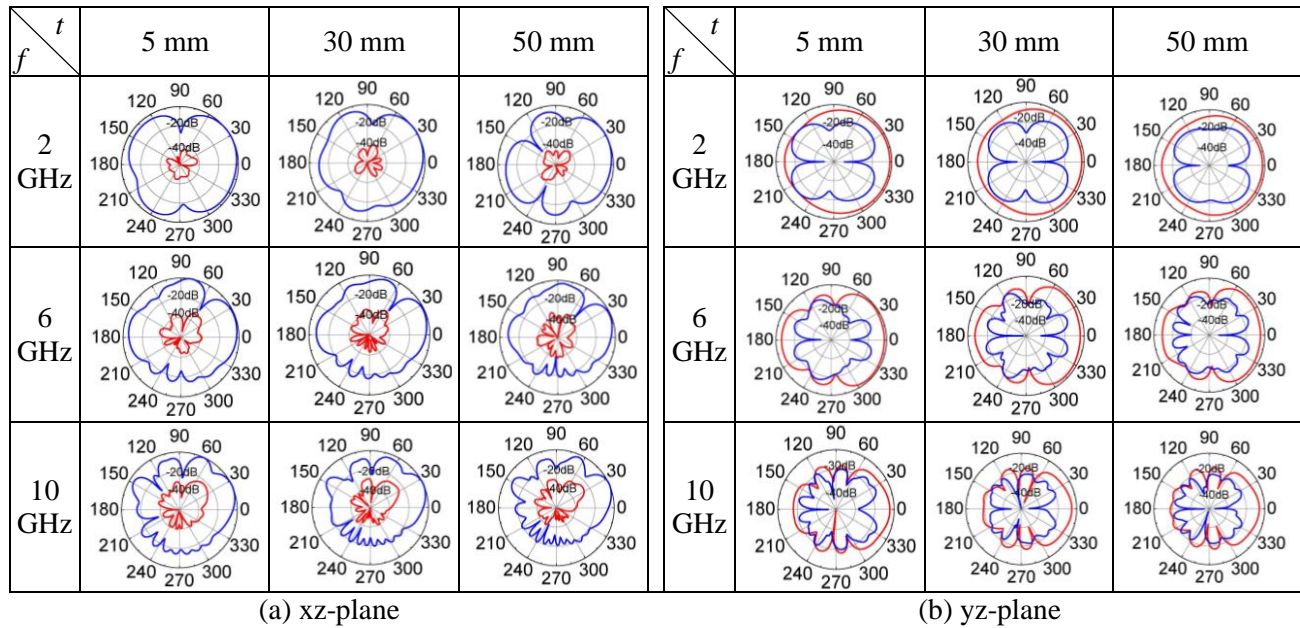


Fig. 12. Effect of the distance  $t$  on radiation pattern (—  $E_\phi$ ; —  $E_\theta$ ).

## V. CONCLUSION

In this paper, a compact halved Vivaldi antenna has been proposed, and the impedance bandwidth and radiation characteristics also have been presented. To obtain wide bandwidth and small size, a dual-exponential edges configuration is selected and a  $100 \Omega$  resistor is integrated at the slot-line end of the proposed antenna. By adjusting each parameter carefully, it is easy to obtain the optimal antenna design and a small size of only  $30 \text{ mm} \times 60.5 \text{ mm}$ . The measured results show that the proposed antenna achieves an impedance bandwidth from 1.44 to 18.5 GHz for  $\text{VSWR} \leq 2.2$ , and has a cross-polarization level of more than 20 dB below the co-polarization level at end-fire direction. Overall, the proposed antenna has small size, low cross-polarization levels, directive radiation and vertically polarized characteristics. All these features make the proposed antenna a good candidate for mounting on metallic surface of a variety of communication systems, such as missile, unmanned aerial vehicles, and the like.

## ACKNOWLEDGMENT

This work is supported by a Project from Science and Technology on Electronic Information Control Laboratory of China under Grant No. M16010101SYSJJ2010-5.

## REFERENCES

- [1] F. Zhang, F. S. Zhang, G. Zhao, C. Lin, and Y. C. Jiao, "A loaded wideband linearly tapered slot antenna with broad beamwidth," *IEEE Antennas and Wireless Propag. Lett.*, vol. 10, pp. 79-82, 2011.
- [2] F. G. Zhu, S. Gao, et al., "Compact-size linearly tapered slot antenna for portable ultra-wideband imaging systems," *Int. J RF Microwave Comput.-Aided Eng.* (2012), first published online.
- [3] D. Schaubert, E. Kollberg, et al., "End-fire tapered slot antennas on dielectric substrates," *IEEE Trans. Antennas Propag.*, vol. 33, no. 12, pp. 1392-1400, 1985.
- [4] N. B. Wang, Y. C. Jiao, Y. Song, L. Zhang, and F. S. Zhang, "A microstrip-fed logarithmically tapered slot antenna for wideband applications," *Journal of Electromagnetic Waves and Applications*, vol. 23, pp. 1335-1344, 2009.
- [5] P. Wang, G. J. Wen, H. B. Zhang, and Y. H. Sun, "A wideband conformal end-fire antenna array mounted on a large conducting cylinder," *IEEE Trans. Antennas Propag.*, vol. 61, no. 9, 2013.
- [6] C. M. Hsu, L. Murphy, T. L. Chin, and E. Arvas, "Vivaldi antenna for GPR," *25<sup>th</sup> Annual Review of Progress in Applied Computational Electromagnetics*, pp. 8-12, California, March 2009.
- [7] B. Zhou, H. Li, X. Y. Zou, and T. J. Cui, "Broadband and high-gain planar vivaldi antennas based on inhomogeneous anisotropic zero-index metamaterials," *Progress In Electromagnetics*

- Research*, vol. 120, pp. 235-247, 2011.
- [8] P. Wang, H. B. Zhang, G. J. Wen, and Y. H. Sun, "Design of modified 6-18 GHz balanced antipodal vivaldi antenna," *Progress In Electromagnetics Research C*, vol. 25, pp. 271-285, 2012.
- [9] P. Wang, G. J. Wen, Y. H. Sun, and H. B. Zhang, "Design of wideband conformal end-fire antenna array on a large conducting cylinder," *2012 IEEE Asia-Pacific Conference on Antennas and Propagation*, pp. 27-29, Singapore, August 2012.
- [10] J. R. Verbiest and G. A. E. Vandenbosch, "Low-cost small-size tapered slot antenna for lower band UWB applications," *Electron. Lett.*, vol. 42, pp. 670-671, 2006.
- [11] J. Shin and D. H. Schaubert, "A parameter study of stripline-fed vivaldi notch-antenna arrays," *IEEE Trans. Antennas Propag.*, vol. 47, no. 5, pp. 879-886, 1999.
- [12] E. W. Reid, L. O. Balbuena, and K. Moez, "Integrated low-loss balun for vivaldi antennas," *Electron. Lett.*, vol. 45, pp. 442-444, 2009.
- [13] E. W. Reid, L. O. Balbuena, A. Ghadiri, and K. Moez, "A 324-element vivaldi antenna array for radio astronomy instrumentation," *IEEE Trans. Instru. Measur.*, vol. 61, no. 1, pp. 241-250, 2012.



**Ping Wang** was born in Chongqing, China, in 1981. He received his B.S. degree in Physics from Western Chongqing University of China, in 2005, and the M.S. degree in Theoretical Physics from Chongqing University, Chongqing, in 2008.

Currently, he is working towards his Ph.D. degree at the University of Electronic Science and Technology of China (UESTC). His current research interests include patch antennas, wideband antennas, and arrays.



**Guangjun Wen** was born in Sichuan, China, in 1964. He received his M.S. and Ph.D. degrees from Chongqing University of China in 1995 and from University of Electronic Science and Technology of China in 1998, respectively. He is currently a

Professor at the University of Electronic Science and Technology of China. His research and industrial experience covers a broad spectrum of electromagnetics, including RF, Microwave, Millimeter wave Integrated Circuits and Systems design, and networks, antennas, as well as, model of electromagnetic metamaterial.



**Yongjun Huang** was born in Sichuan, China, in 1985. Currently, he is working towards his Ph.D. degree at the University of Electronic Science and Technology of China (UESTC). His research interests include electromagnetic metamaterial and its application in

microwave engineering area, FDTD analysis for the model and RCS characteristic of metamaterials.

**Haobin Zhang** received his Ph.D degree in Northwest Polytechnical University, China. Currently, he is working at Science and Technology on Electronic Information Control Laboratory of China. His research interests include analytical and numerical modeling of antenna, and antenna theory and design.